

## Supplementary Information

### **KCl-assisted activation: Moringa oleifera branch-derived porous carbon for high performance supercapacitor**

Yongxiang Zhang<sup>a,b</sup>, Peifeng Yu<sup>a</sup>, Mingtao Zheng<sup>a,b</sup>, Yong Xiao<sup>a,b</sup>, Hang Hu<sup>a,b</sup>, Yeru Liang<sup>a,b</sup>, Yingliang Liu<sup>a,b\*</sup>, Hanwu Dong<sup>a,b\*</sup>

<sup>a</sup> Key Laboratory for Biobased Materials and Energy of Ministry of Education, College of Materials and Energy, South China Agricultural University, Guangzhou, 510642, Guangdong, China

<sup>b</sup> Guangdong Laboratory of Lingnan Modern Agriculture, Guangzhou, 510642, China

*E-mail address:* hanwu@scau.edu.cn; tliuyl@scau.edu.cn.

### **Supporting Information Contents:**

Number of pages: 16

Number of figures: 11

Number of tables: 10

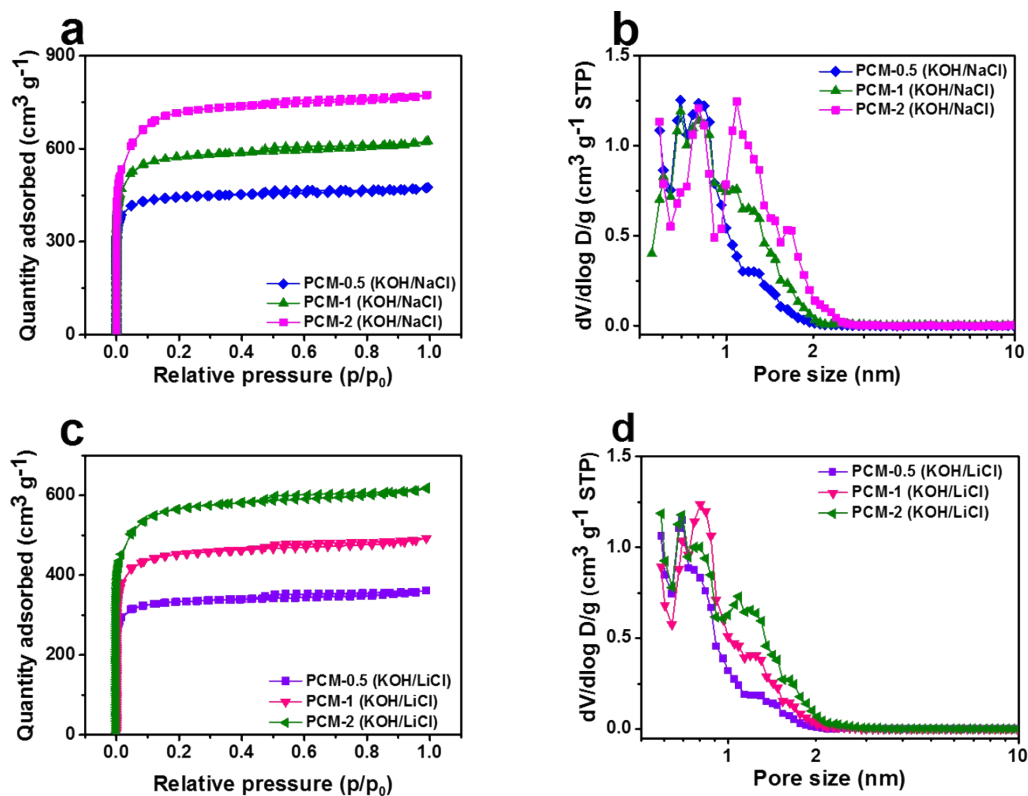


**Figure S1.** (a) N<sub>2</sub> adsorption-desorption isotherms, (b) DFT pore size distribution curves of PCM-0.5 (KOH/NaCl), PCM-1 (KOH/NaCl) and PCM-2 (KOH/NaCl). (c) N<sub>2</sub> adsorption-desorption isotherms, (d) DFT pore size distribution curves of PCM-0.5 (KOH/LiCl), PCM-1 (KOH/LiCl) and PCM-2 (KOH/LiCl).

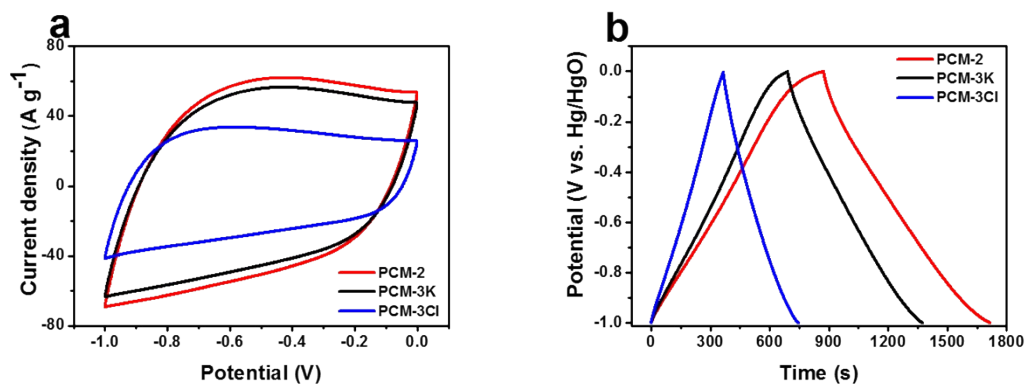


**Figure S2.** Comparison of (a) CV curves at 200 mV s<sup>-1</sup> and (b) GCD curves at 0.5 A g<sup>-1</sup> for PCM-2, PCM-3K and PCM-3Cl in a three-electrode system by using 6.0 M KOH aqueous solution as the electrolyte.

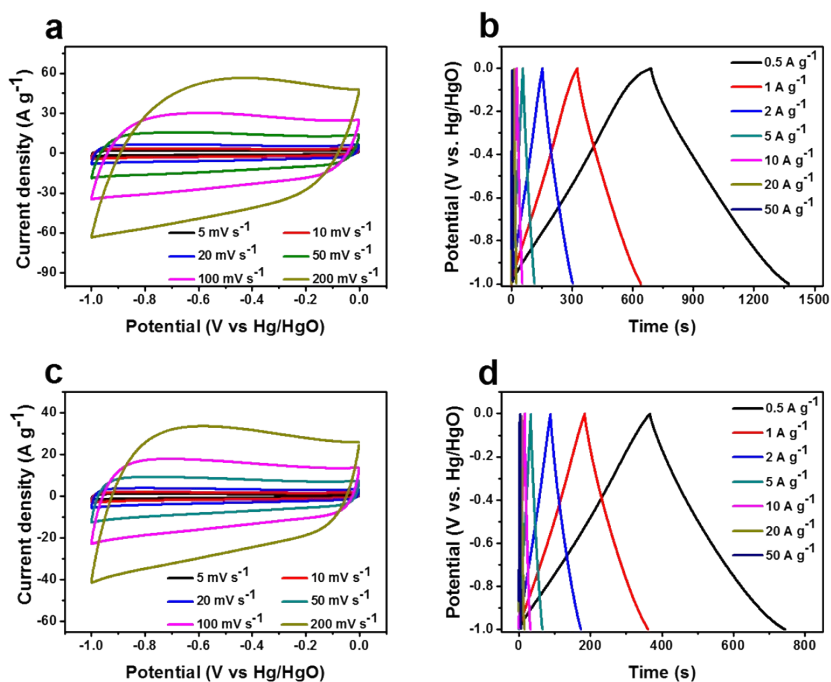


**Figure S3.** CV and GCD curves of (a, b) PCM-3K and (c, d) PCM-3Cl in a three-electrode system by using 6.0 M KOH aqueous solution as the electrolyte.

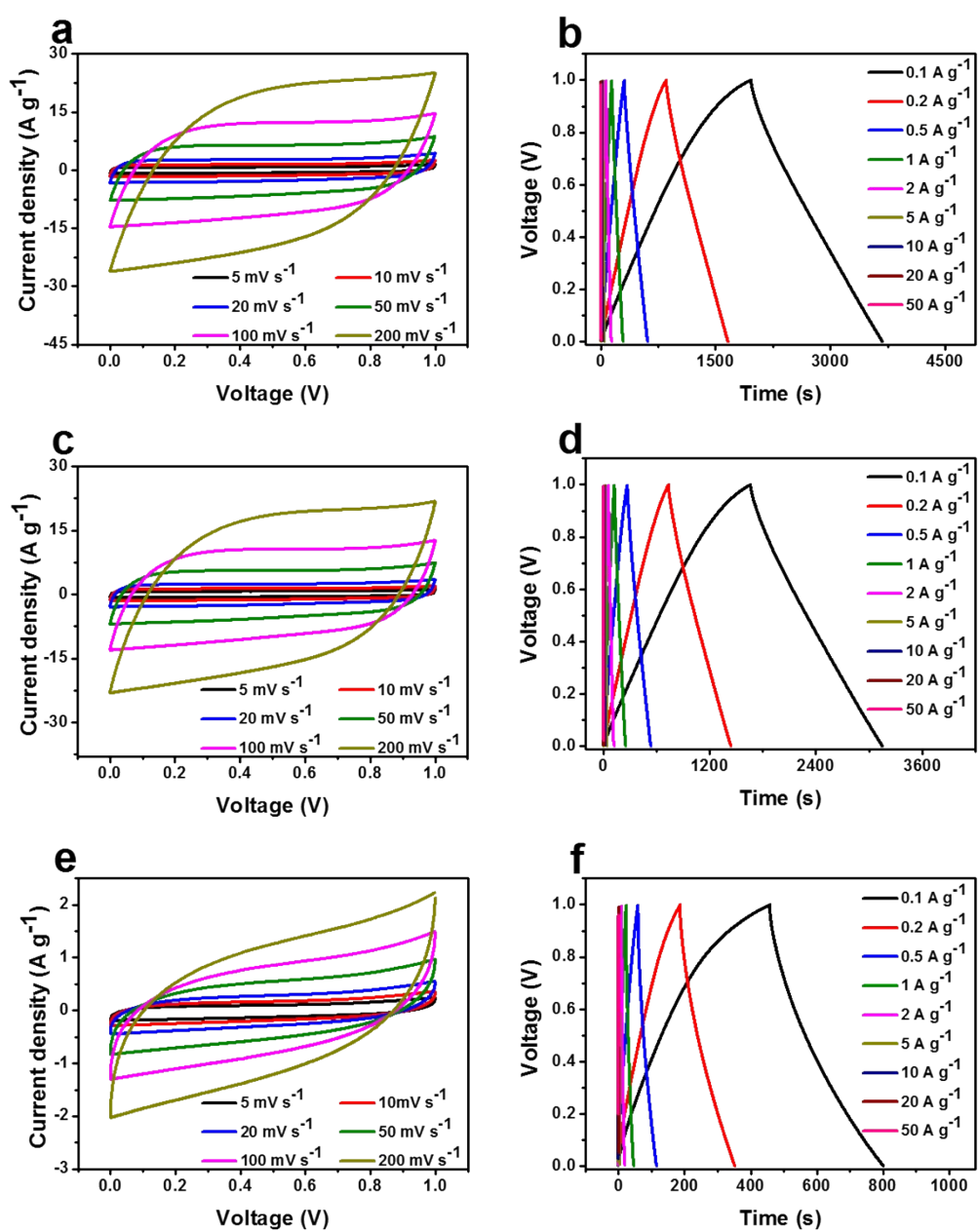


**Figure S4.** CV and GCD curves of (a, b) PCM-2, (c, d) PCM-3K and (e, f) PCM-3Cl coin-type symmetrical supercapacitors by using 6 M KOH aqueous solution as electrolyte.

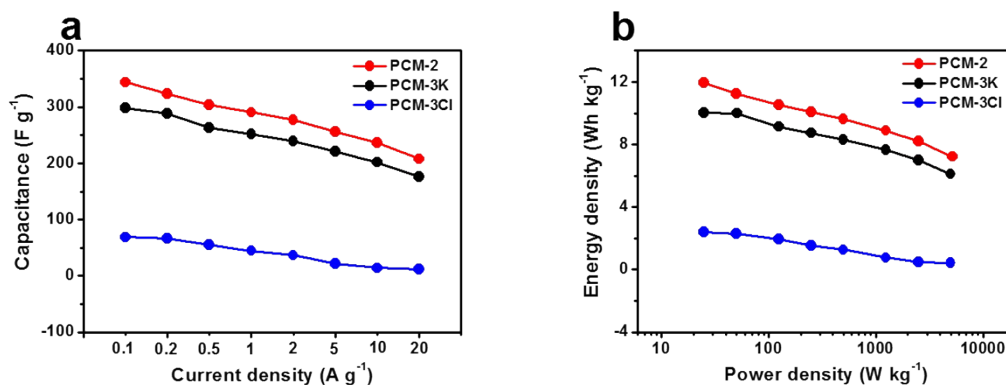


**Figure S5.** (a) Capacitance comparison of PCM-2, PCM-3K and PCM-3Cl at various current densities in a coin-type supercapacitor and (b) Ragone plots of sample in coin-type supercapacitors by using 6.0 M KOH aqueous solution as the electrolyte.

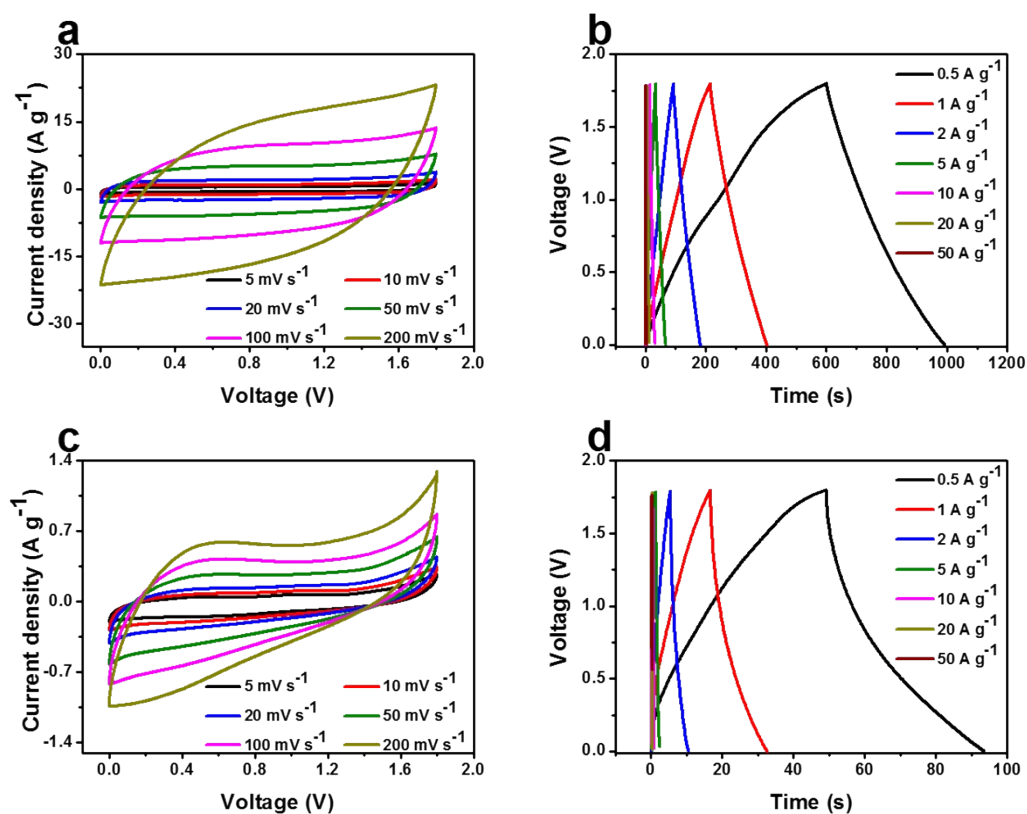


**Figure S6.** CV and GCD curves of (a, b) PCM-3K and (c, d) PCM-3Cl coin-type symmetrical supercapacitors by using 1.0 M Na<sub>2</sub>SO<sub>4</sub> aqueous solution as electrolyte.

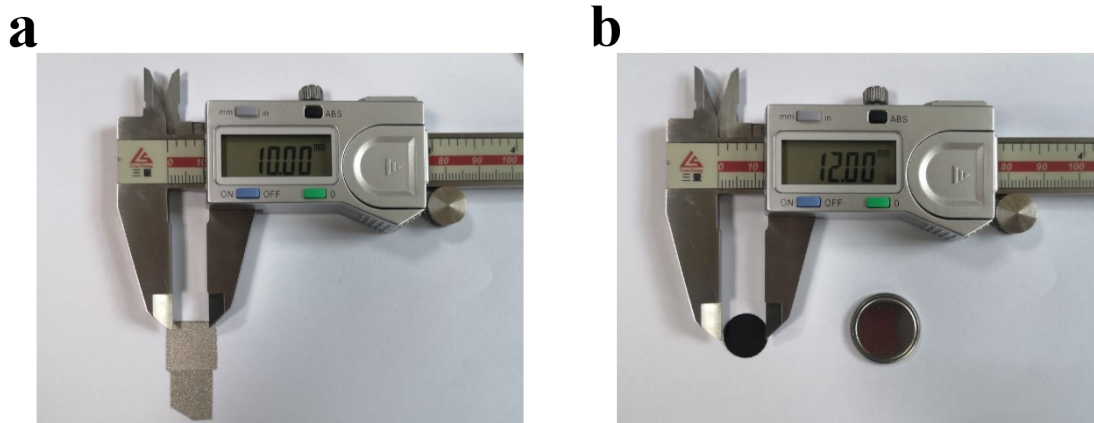


**Figure S7.** (a) The size dimension of PCMs electrode for the three-electrode system ( $1 \times 1 \text{ cm}^2$ ), (b) The size dimension of the PCMs electrode for the two-electrode symmetrical supercapacitors ( $0.36\pi \text{ cm}^2$ ).

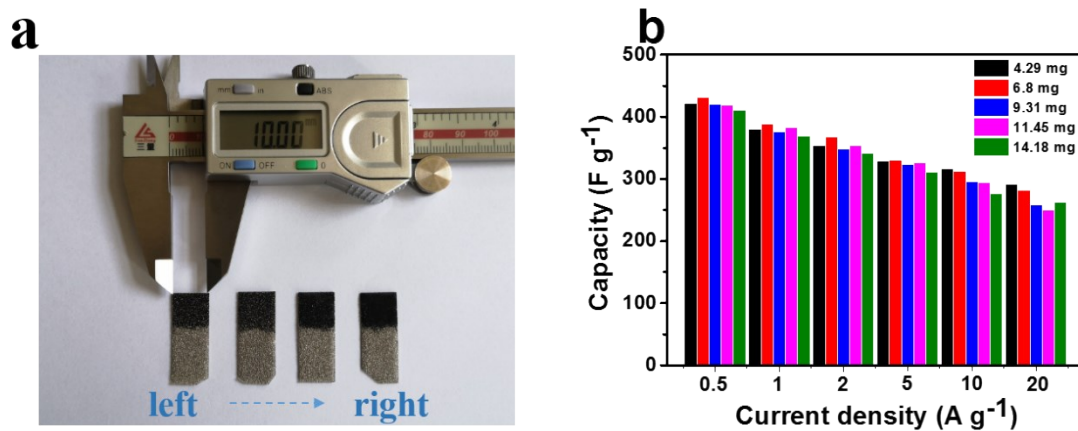


**Figure S8.** (a) The PCM-2-based electrodes loaded with different masses (the loading masses from left to right are 6.8, 9.31, 11.45 and 14.18  $\text{mg cm}^{-2}$  (including active materials, carbon black, PTFE and the mass ratio is 8:1:1), respectively). (b) The gravimetric capacitance of PCM-2-base electrodes loaded with different masses.

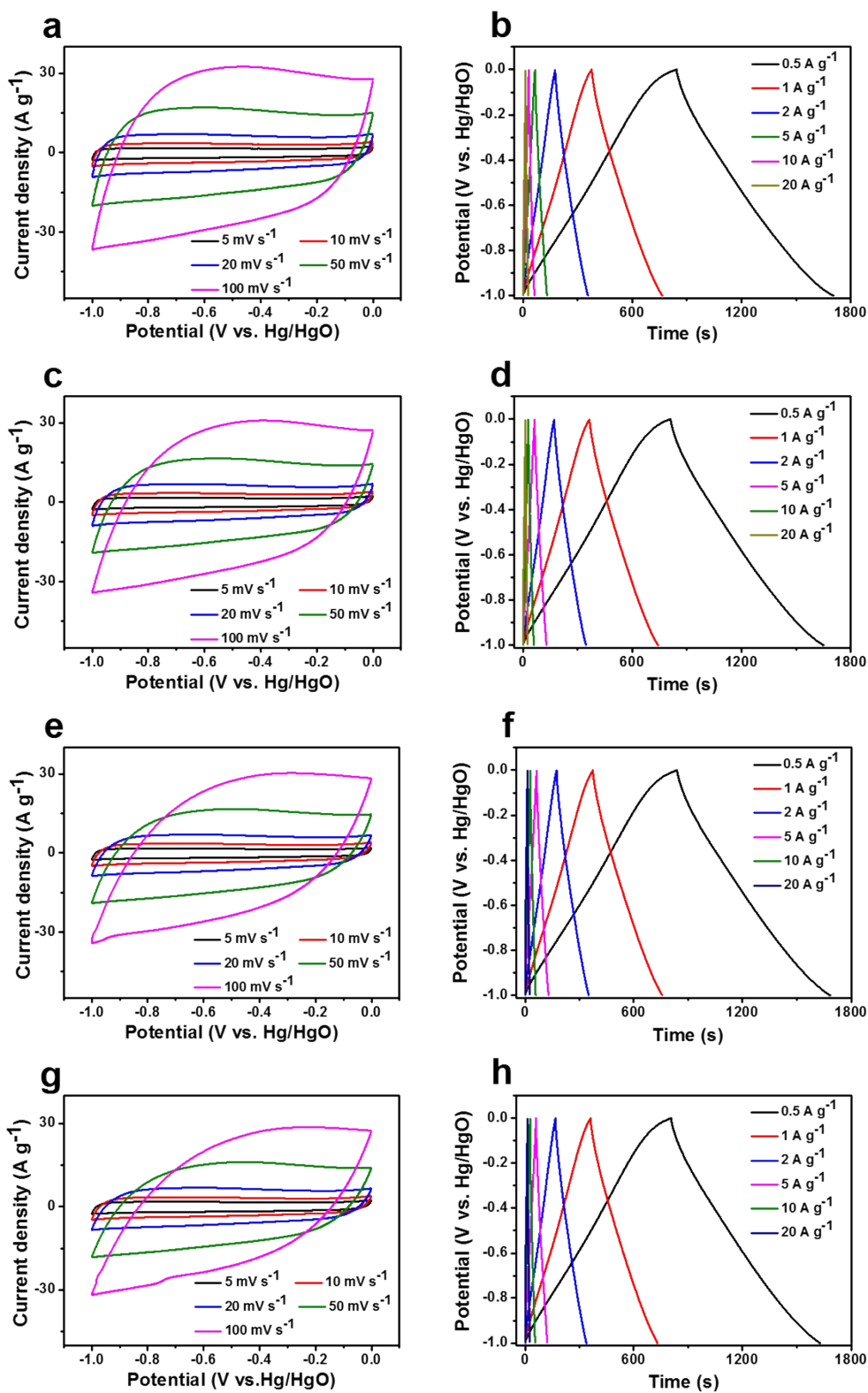


Figure S9. CV and GCD curves of PCM-2 electrodes loaded with different masses in a three-electrode system by using 6.0 M KOH aqueous solution as the electrolyte. (a, b) 6.8, (c, d) 9.31, (e, f) 11.45 and (g, h) 14.18 mg cm<sup>-2</sup>.

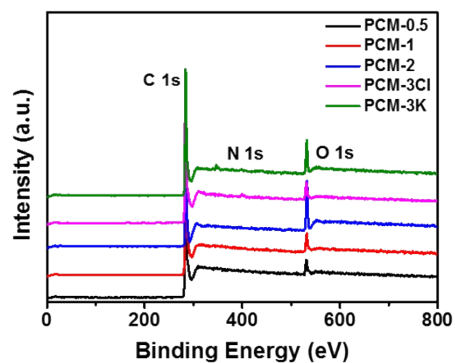
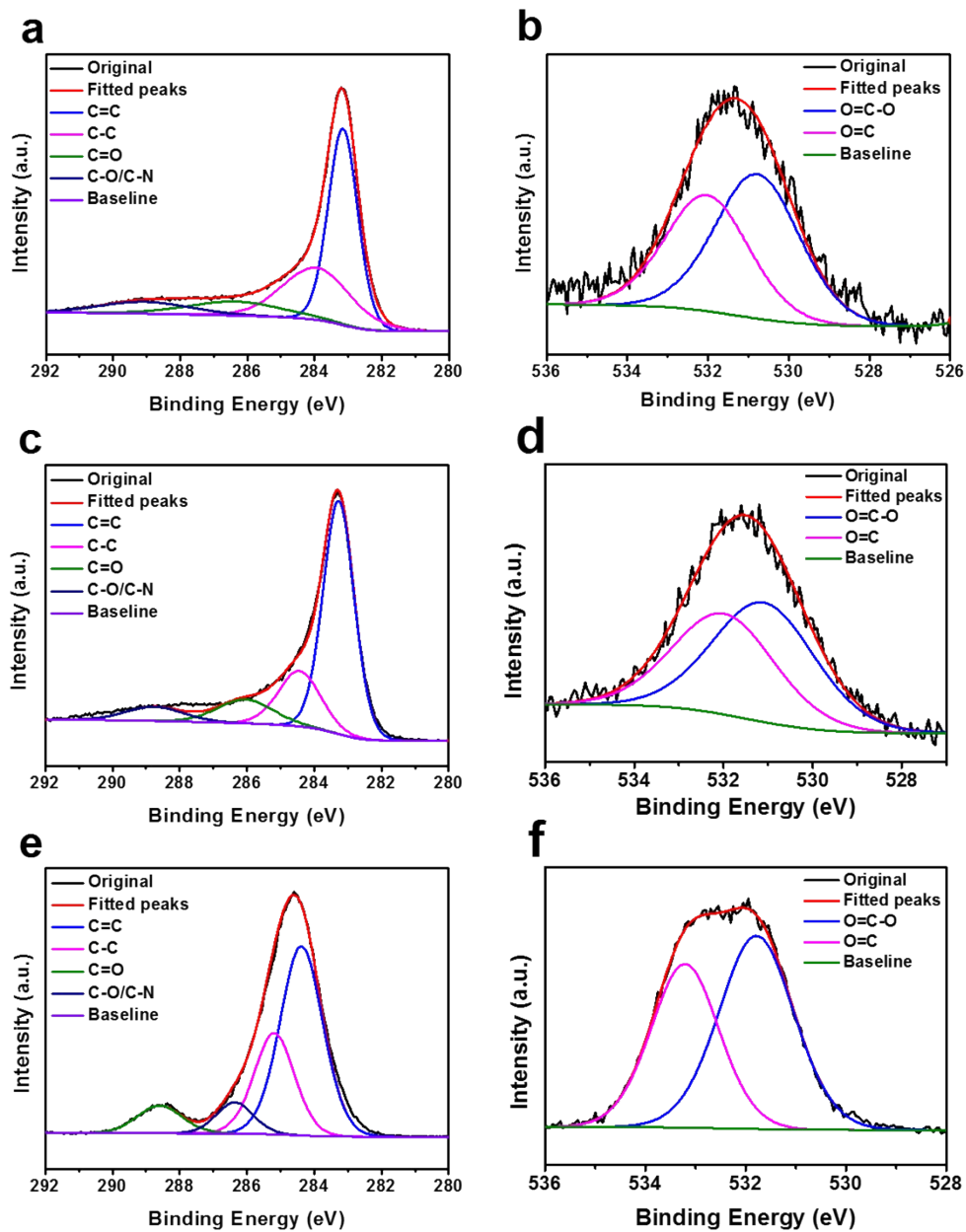


Figure S10. XPS spectra of the as-prepared PCM-0.5, PCM-1, PCM-2, PCM-3Cl and PCM-3K.





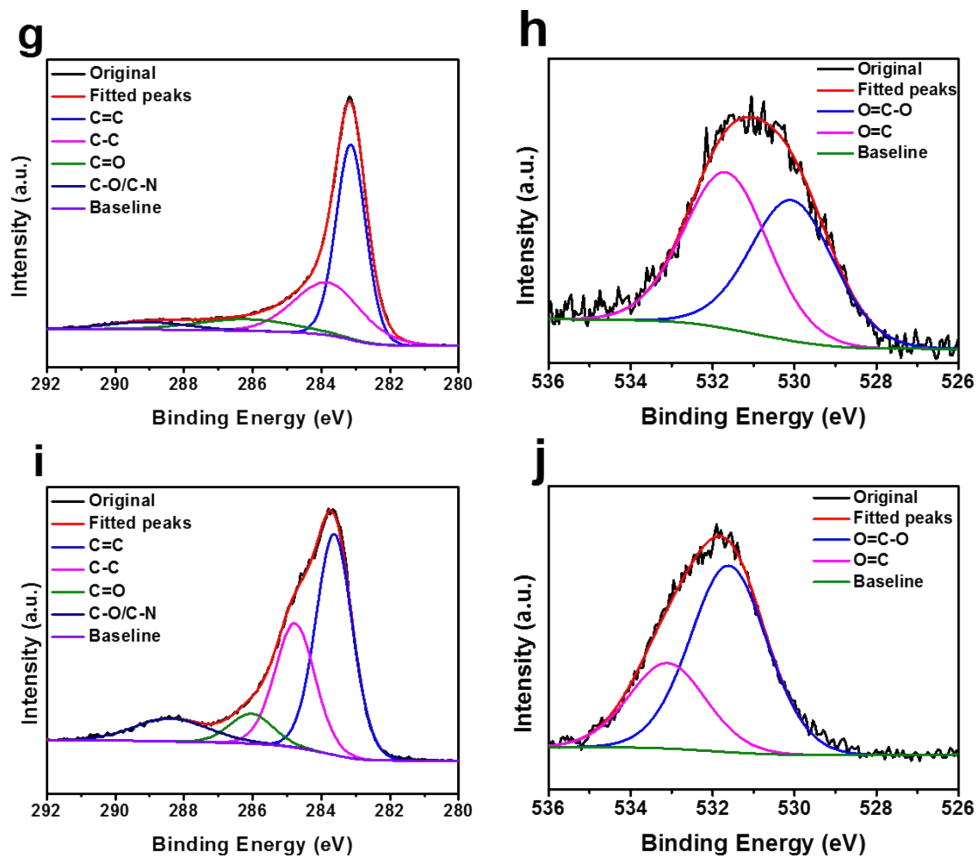


Figure S11. High-resolution C 1s and O 1s XPS spectra of (a, b) PCM-0.5, (c, d) PCM-1, (e, f) PCM-2, (g, h) PCM-3Cl and (i, j) PCM-3K.

**Table S1.** Summary of textural characteristics of as-prepared samples (KOH/KCl).

Sample	<sup>a</sup> S <sub>BET</sub> (m <sup>2</sup> g <sup>-1</sup> )	<sup>b</sup> S <sub>mic</sub> (m <sup>2</sup> g <sup>-1</sup> )	<sup>c</sup> V <sub>t</sub> (cm <sup>3</sup> g <sup>-1</sup> )	<sup>d</sup> V <sub>mic</sub> (cm <sup>3</sup> g <sup>-1</sup> )	<sup>e</sup> Biomass yields (%)
PCM-3Cl	927	861	0.38	0.33	17.5
PCM-0.5	2314	2166	0.94	0.84	15.6
PCM-1	2703	2546	1.15	1.03	14.6
PCM-2	3470	2786	1.69	1.16	12.5
PCM-3K	3389	2481	1.67	1.03	9.8

**Table S2.** Summary of textural characteristics of as-prepared samples (KOH/NaCl).

Sample	<sup>a</sup> S <sub>BET</sub> (m <sup>2</sup> g <sup>-1</sup> )	<sup>b</sup> S <sub>mic</sub> (m <sup>2</sup> g <sup>-1</sup> )	<sup>c</sup> V <sub>t</sub> (cm <sup>3</sup> g <sup>-1</sup> )	<sup>d</sup> V <sub>mic</sub> (cm <sup>3</sup> g <sup>-1</sup> )
PCM-0.5 (KOH/NaCl)	1759	1639	0.73	0.63
PCM-1 (KOH/NaCl)	2219	2069	0.95	0.81
PCM-2 (KOH/NaCl)	2697	2477	1.19	1.0

**Table S3.** Summary of textural characteristics of as-prepared samples (KOH/LiCl).

Sample	<sup>a</sup> S <sub>BET</sub> (m <sup>2</sup> g <sup>-1</sup> )	<sup>b</sup> S <sub>mic</sub> (m <sup>2</sup> g <sup>-1</sup> )	<sup>c</sup> V <sub>t</sub> (cm <sup>3</sup> g <sup>-1</sup> )	<sup>d</sup> V <sub>mic</sub> (cm <sup>3</sup> g <sup>-1</sup> )
PCM-0.5 (KOH/LiCl)	1325	1228	0.55	0.47
PCM-1 (KOH/LiCl)	1767	1641	0.75	0.64
PCM-2 (KOH/LiCl)	2169	1741	0.94	0.69

(a) Specific surface area.

(b) Micropore surface area.

(c) Total pore volume.

(d) Micropore volume.

(e) The yield of the porous carbon based on raw materials.

**Table S4.** The specific surface areas and preparation conditions of porous carbon derived from different precursors reported in the literatures.

Carbon precursors	S <sub>BET</sub> (m <sup>2</sup> g <sup>-1</sup> )	S <sub>micro</sub> (m <sup>2</sup> g <sup>-1</sup> )	T (°C)	Activation agent	Ref.
Soybean milk powder	1208	987	700	KOH/CaCO <sub>3</sub>	[1]
Mung bean husks	1278	1057	700	KOH	[2]
Tannic acid	1570	1333	800	NaCl/ZnCl <sub>2</sub>	[3]
Ripe plane tree fluff	1416	995	800	KOH/FeNO <sub>3</sub>	[4]
Petroleum asphalt	2227	1741	900	KOH/NaCl/KCl	[5]
Rice straw	2646	1416	800	KOH	[6]
Wild jujube pit powder	2438	2170	800	KOH	[7]
Eulaliopsis binata	2273	1045	850	KOH	[8]
Puffed rice	3326	2193	850	KOH	[9]
Miscellaneous wood fibers	1807	1743.5	800	KOH	[10]
Wax gourd	2544	1747	800	KOH	[11]
Camellia oleifera	1726	858	800	KOH	[12]
Rhus typhina	2676	2354	800	KOH	[13]
Stachyurus Chinensis Franch	1994	647.6	800	KOH	[14]
Corncob sponge	1909	1209	850	KOH	[15]
Fallen leaves	1409	791	700	KOH/K <sub>2</sub> CO <sub>3</sub>	[16]
D- (+)-glucose	1500	1440	700	KOH/ZnCl <sub>2</sub>	[17]
<b>Moringa oleifera branch</b>	<b>3470</b>	<b>2786</b>	<b>800</b>	<b>KOH/KCl</b>	<b>This work</b>

**Table S5.** The detailed element content of C, N, and O.

Sample	C <sub>total</sub> (%)	N <sub>total</sub> (%)	O <sub>total</sub> (%)
PCM-0.5	94.1	0.85	5.05
PCM-1	92.94	1.12	5.94
PCM-2	84.18	0.85	14.97
PCM-3Cl	92.43	2.03	5.54
PCM-3K	88.67	1.37	9.97

**Table S6.** Electrochemical performance of Moringa oleifera branch-derived porous carbon in three-electrode system (6 mol L<sup>-1</sup> KOH and current density of 0.5 A g<sup>-1</sup>).

Sample	Active material (mg)	Area (cm <sup>2</sup> )	Gravimetric capacitance (F g <sup>-1</sup> )	Areal capacitance (mF cm <sup>-2</sup> )
PCM-2	3.43	1	421	1444
PCM-3K	3.48	1	340	1183
PCM-3Cl	3.42	1	189	645

**Table S7.** Electrochemical performance of Moringa oleifera branch-derived porous carbon in two-electrode system (6 mol L<sup>-1</sup> KOH and current density of 0.1 A g<sup>-1</sup>).

Sample	Active material (mg)	Area (cm <sup>2</sup> )	Gravimetric capacitance (F g <sup>-1</sup> )	Areal capacitance (mF cm <sup>-2</sup> )
PCM-2	3.45//3.47	0.36 $\pi$	343.8	1052
PCM-3K	3.04//3.11	0.36 $\pi$	297.8	808

**Table S8.** Electrochemical performance of Moringa oleifera branch-derived porous carbon in two-electrode system (1 mol L<sup>-1</sup> Na<sub>2</sub>SO<sub>4</sub> and current density of 0.5 A g<sup>-1</sup>).

Sample	Active material (mg)	Area (cm <sup>2</sup> )	Gravimetric capacitance (F g <sup>-1</sup> )	Areal capacitance (mF cm <sup>-2</sup> )
PCM-2	3.24//3.29	0.36 $\pi$	293.7	848
PCM-3K	3.45//3.58	0.36 $\pi$	195.5	607.9

**Table S9.** The comparison of electrochemical performance between *Moringa oleifera* branch and carbon materials electrodes reported in 6 M KOH electrolyte system.

Carbon precursors	Capacitance (F g <sup>-1</sup> )		Current density (A g <sup>-1</sup> )	Ref.
	Ref	This work		
Reed membranes	353.6	<b>421</b>	0.5	[18]
Silicone resin	322	<b>421</b>	0.5	[19]
Waste bones	302	<b>421</b>	0.5	[20]
Sucrose	302	<b>380</b>	1	[21]
Nanoporous graphene	204	<b>316</b>	10	[22]
D (+)-glucosamine	388	<b>421</b>	0.5	[23]
Rose	208	<b>421</b>	0.5	[24]
Bagasse	320	<b>421</b>	0.5	[25]
Cotton stalk	282	<b>421</b>	0.5	[26]
Polyacrylonitrile	331	<b>421</b>	0.5	[27]
Sewage sludge	379	<b>421</b>	0.5	[28]
Cigarette butt	330.1	<b>421</b>	0.5	[29]
Tobacco rods	286.6	<b>421</b>	0.5	[30]
Black locust seed dregs	333	<b>380</b>	1	[31]
Celery	245	<b>421</b>	0.5	[32]
Perilla frutescens leaves	270	<b>421</b>	0.5	[33]
Willow catkins	231	<b>316</b>	10	[34]
<i>Moringa oleifera</i> stem	283	<b>421</b>	0.5	[35]

**Table S10.** The comparison of electrochemical performance for representative carbons in 1 M Na<sub>2</sub>SO<sub>4</sub> electrolyte system.

Carbon precursors	Capacitance (F g <sup>-1</sup> )	Current density (A g <sup>-1</sup> )	Ref.
N, S-Doped porous carbon	204	0.5	[36]
1D carbon nanobelts //MnO <sub>2</sub>	265	0.2	[37]
3D Porous carbon nanosheet	230	0.5	[38]
Polyacrylonitrile based porous carbon	218	0.5	[39]
Graphene-like porous carbon	255	0.5	[40]
Hierarchical porous carbon	211	0.5	[41]
Three-dimensional porous carbon	179	0.5	[42]
Nitrogen-doped porous carbon	134	1	[43]
Microporous active carbon	138	1	[44]
Honeycomb-like porous carbon	212	0.5	[45]
Hierarchical porous carbon	186	0.5	[46]
Hierarchical porous carbon	191	0.5	[47]
Carbon nanosheets	272	1	[35]
N, O-enriched porous carbons	157	0.2	[48]
Egg-Box-Like porous carbon	181	0.2	[49]
N/O co-doped carbon	328	0.2	[50]
Porous carbon	206	0.5	[51]
<b>PCM-2</b>	<b>293.7</b>	<b>0.5</b>	<b>This work</b>

## References:

1. M. Chen, D. Yu, X. Zheng and X. Dong, *Journal of Energy Storage*, 2019, **21**, 105-112.
2. M. Song, Y. Zhou, X. Ren, J. Wan, Y. Du, G. Wu and F. Ma, *J Colloid Interface Sci*, 2019, **535**, 276-286.
3. G. A. Tiruye, D. Muñoz-Torrero, T. Berthold, J. Palma, M. Antonietti, N. Fechler and R. Marcilla, *Journal of Materials Chemistry A*, 2017, **5**, 16263-16272.
4. Y. Yao, Y. Zhang, L. Li, S. Wang, S. Dou and X. Liu, *ACS Appl Mater Interfaces*, 2017, **9**, 34944-34953.
5. L. Pan, X. Li, Y. Wang, J. Liu, W. Tian, H. Ning and M. Wu, *Applied Surface Science*, 2018, **444**, 739-746.
6. L. Zhu, F. Shen, R. L. Smith, L. Yan, L. Li and X. Qi, *Chemical Engineering Journal*, 2017, **316**, 770-777.
7. K. Sun, S. Yu, Z. Hu, Z. Li, G. Lei, Q. Xiao and Y. Ding, *Electrochimica Acta*, 2017, **231**, 417-428.
8. B. Liu, H. Chen, Y. Gao and H. Li, *Electrochimica Acta*, 2016, **189**, 93-100.
9. J. Hou, K. Jiang, M. Tahir, X. Wu, F. Idrees, M. Shen and C. Cao, *Journal of Power Sources*, 2017, **371**, 148-155.
10. F. Liu, Y. Gao, C. Zhang, H. Huang, C. Yan, X. Chu, Z. Xu, Z. Wang, H. Zhang, X. Xiao and W. Yang, *J Colloid Interface Sci*, 2019, **548**, 322-332.
11. X. Bo, K. Xiang, Y. Zhang, Y. Shen, S. Chen, Y. Wang, M. Xie and X. Guo, *Journal of Energy Chemistry*, 2019, **39**, 1-7.
12. D. Yu, Y. Ma, M. Chen and X. Dong, *J Colloid Interface Sci*, 2019, **537**, 569-578.
13. X. Wei, J.-S. Wei, Y. Li and H. Zou, *Journal of Power Sources*, 2019, **414**, 13-23.
14. Y. Yao, Z. Xiao, P. Liu, S. Zhang, Y. Niu, H. Wu, S. Liu, W. Tu, Q. Luo, M. A. Z. G. Sial, S. Zeng, Q. Zhang, J. Zou, X. Zeng and W. Zhang, *Carbon*, 2019, **155**, 674-685.
15. L. Peng, Y. Liang, H. Dong, H. Hu, X. Zhao, Y. Cai, Y. Xiao, Y. Liu and M. Zheng, *Journal of Power Sources*, 2018, **377**, 151-160.
16. Y.-T. Li, Y.-T. Pi, L.-M. Lu, S.-H. Xu and T.-Z. Ren, *Journal of Power Sources*, 2015, **299**, 519-528.
17. M. Härmas, T. Thomberg, H. Kurig, T. Romann, A. Jänes and E. Lust, *Journal of Power Sources*, 2016, **326**, 624-634.
18. C.-L. Ban, Z. Xu, D. Wang, Z. Liu and H. Zhang, *ACS Sustainable Chemistry & Engineering*, 2019, **7**, 10742-10750.
19. J. Yang, J. Hu, M. Zhu, Y. Zhao, H. Chen and F. Pan, *Journal of Power Sources*, 2017, **365**, 362-371.
20. L. Niu, C. Shen, L. Yan, J. Zhang, Y. Lin, Y. Gong, C. Li, C. Q. Sun and S. Xu, *J Colloid Interface Sci*, 2019, **547**, 92-101.
21. J. Zhou, M. Wang and X. Li, *Applied Surface Science*, 2018, **462**, 444-452.
22. E. Senthilkumar, V. Sivasankar, B. R. Kohakade, K. Thileepkumar, M. Ramya, G. Sivagaami Sundari, S. Raghu and R. A. Kalaivani, *Applied Surface Science*, 2018, **460**, 17-24.
23. Y. Qing, Y. Jiang, H. Lin, L. Wang, A. Liu, Y. Cao, R. Sheng, Y. Guo, C. Fan, S. Zhang, D. Jia and Z. Fan, *Journal of Materials Chemistry A*, 2019, **7**, 6021-6027.
24. C. Zhao, Y. Huang, C. Zhao, X. Shao and Z. Zhu, *Electrochimica Acta*, 2018, **291**, 287-296.
25. H. Feng, H. Hu, H. Dong, Y. Xiao, Y. Cai, B. Lei, Y. Liu and M. Zheng, *Journal of Power Sources*, 2016, **302**, 164-173.
26. Z. Li, S. Gao, H. Mi, C. Lei, C. Ji, Z. Xie, C. Yu and J. Qiu, *Carbon*, 2019, **149**, 273-280.
27. Y. Liu, N. Liu, L. Yu, X. Jiang and X. Yan, *Chemical Engineering Journal*, 2019, **362**, 600-608.
28. H. Feng, M. Zheng, H. Dong, Y. Xiao, H. Hu, Z. Sun, C. Long, Y. Cai, X. Zhao, H. Zhang, B. Lei and Y. Liu, *Journal of Materials Chemistry A*, 2015, **3**, 15225-15234.
29. Q. Meng, W. Chen, L. Wu, J. Lei, X. Liu, W. Zhu and T. Duan, *Energy*, 2019, **189**, 116241.
30. Y.-Q. Zhao, M. Lu, P.-Y. Tao, Y.-J. Zhang, X.-T. Gong, Z. Yang, G.-Q. Zhang and H.-L. Li, *Journal of Power Sources*, 2016, **307**, 391-400.

31. L. Hou, Z. Hu, X. Wang, L. Qiang, Y. Zhou, L. Lv and S. Li, *J Colloid Interface Sci*, 2019, **540**, 88-96.
32. J. He, D. Zhang, M. Han, X. Liu, Y. Wang, Y. Li, X. Zhang, K. Wang, H. Feng and Y. Wang, *Journal of Energy Storage*, 2019, **21**, 94-104.
33. B. Liu, Y. Liu, H. Chen, M. Yang and H. Li, *Journal of Power Sources*, 2017, **341**, 309-317.
34. K. Wang, N. Zhao, S. Lei, R. Yan, X. Tian, J. Wang, Y. Song, D. Xu, Q. Guo and L. Liu, *Electrochimica Acta*, 2015, **166**, 1-11.
35. Y. Cai, Y. Luo, H. Dong, X. Zhao, Y. Xiao, Y. Liang, H. Hu, Y. Liu and M. Zheng, *Journal of Power Sources*, 2017, **353**, 260-269.
36. D. Wu, J. Cheng, T. Wang, P. Liu, L. Yang and D. Jia, *ACS Sustainable Chemistry & Engineering*, 2019, **7**, 12138-12147.
37. T. Ouyang, K. Cheng, F. Yang, L. Zhou, K. Zhu, K. Ye, G. Wang and D. Cao, *Journal of Materials Chemistry A*, 2017, **5**, 14551-14561.
38. Y. Li, S. Liu, Y. Liang, Y. Xiao, H. Dong, M. Zheng, H. Hu and Y. Liu, *ACS Sustainable Chemistry & Engineering*, 2019, **7**, 13827-13835.
39. Y. Li, Y. Liang, H. Hu, H. Dong, M. Zheng, Y. Xiao and Y. Liu, *Carbon*, 2019, **152**, 120-127.
40. G. Yuan, H. Li, H. Hu, Y. Xie, Y. Xiao, H. Dong, Y. Liang, Y. Liu and M. Zheng, *Electrochimica Acta*, 2019, **326**, 134974.
41. J. Huang, L. Chen, H. Dong, Y. Zeng, H. Hu, M. Zheng, Y. Liu, Y. Xiao and Y. Liang, *Electrochimica Acta*, 2017, **258**, 504-511.
42. W. Zhao, Y. Zhu, L. Zhang, Y. Xie and X. Ye, *Journal of Alloys and Compounds*, 2019, **787**, 1-8.
43. C. Long, J. Zhuang, Y. Xiao, M. Zheng, H. Hu, H. Dong, B. Lei, H. Zhang and Y. Liu, *Journal of Power Sources*, 2016, **310**, 145-153.
44. X. Song, X. Ma, Y. Li, L. Ding and R. Jiang, *Applied Surface Science*, 2019, **487**, 189-197.
45. T. Guan, J. Zhao, G. Zhang, J. Wang, D. Zhang and K. Li, *ACS Sustainable Chemistry & Engineering*, 2018, **7**, 2116-2126.
46. J. Huang, Y. Liang, H. Hu, S. Liu, Y. Cai, H. Dong, M. Zheng, Y. Xiao and Y. Liu, *Journal of Materials Chemistry A*, 2017, **5**, 24775-24781.
47. Y. Li, B. Mou, Y. Liang, H. Dong, M. Zheng, Y. Xiao and Y. Liu, *ACS Sustainable Chemistry & Engineering*, 2019, **7**, 15259-15266.
48. Y. Cheng, B. Li, Y. Huang, Y. Wang, J. Chen, D. Wei, Y. Feng, D. Jia and Y. Zhou, *Applied Surface Science*, 2018, **439**, 712-723.
49. Y. Cai, Y. Luo, Y. Xiao, X. Zhao, Y. Liang, H. Hu, H. Dong, L. Sun, Y. Liu and M. Zheng, *ACS Appl Mater Interfaces*, 2016, **8**, 33060-33071.
50. D. He, J. Niu, M. Dou, J. Ji, Y. Huang and F. Wang, *Electrochimica Acta*, 2017, **238**, 310-318.
51. P. Yu, Y. Liang, H. Dong, H. Hu, S. Liu, L. Peng, M. Zheng, Y. Xiao and Y. Liu, *ACS Sustainable Chemistry & Engineering*, 2018, **6**, 15325-15332.